Pseudo-Log-Polar Fourier Transform for Image Registration

Hanzhou Liu, Baolong Guo, and Zongzhe Feng

***Abstract*—A new registration algorithm based on pseudo-log-polar Fourier transform (PLPFT) for estimating large translations, rotations, and scalings in images is developed. The PLPFT, which is calculated at points distributed at nonlinear increased concentric squares, approximates log-polar Fourier representations of images accurately. In addition, it can be calculated quickly by utilizing the Fourier separability property and the fractional fast Fourier transform. Using the log-polar Fourier representations and cross-power spectrum method, we can estimate the rotations and scalings in images and obtain translations later. Experimental results have verified the robustness and high accuracy of this algorithm.**

***Index Terms*—Fractional fast Fourier transform (FFT), image registration, pseudo-log-polar.**

I. Introduction

IMAGE registration represents a vital preprocessing step to many image processing tasks, such as machine vision, medical image processing, and remote sensing [1]. This problem was analyzed by various computational techniques, such as control points, curves, gradient, correlation techniques, mutual information, and discrete Fourier domain algorithms.

In the Fourier domain, all the conventional algorithms [2], [3] are using the two-dimensional (2-D) fast Fourier transform (FFT) to estimate the discrete Fourier transform (DFT) on the polar or log-polar grid. A substantial improved approximation using the pseudo-polar Fourier transform (PPFT) [4] to approximate log-polar Fourier transform was proposed by Keller, and robust detect ability has been obtained for arbitrary angles and large scales. Since the magnitude of 2-D Fourier transform of an image shows itself as a ripple pinnacle, only PPFT will not give accurate DFT values at the low coefficient of the log-polar grid. This limits the ability to detect scales and angles between images.

In this letter, we propose to estimate the log-polar DFT using the pseudo-log-polar Fourier transform (PLPFT). The basic idea is the same as PPFT [6], [7]. The PLPFT estimates the DFT on a non-Cartesian grid, which is geometrically similar to the log-polar grid. In the Cartesian coordinates system, the PLP grid is dense at low coefficients and sparse at high coefficients. This character matches well with the ripple pinnacle peculiarity of Fourier magnitude of images. By utilizing the PLPFT, a significantly smaller interpolation error is achieved at low log-polar coefficients, but this is very big when using the state-of-the-art algorithms.

This letter is organized as follows. In Section II, we introduce the basic registration theory on the Fourier domain. In Section III, we present the pseudo-log-polar Fourier transform. In Section IV, we calculate the log-polar Fourier transform. The registration algorithm and experimental results are presented in Sections V and VI, respectively. In Section VII, we conclude the letter.

II. Basic Theory on Fourier Domain

On the basis of translation, rotation, and scale invariant property of DFT, we can use the log-polar Fourier representation to register images that are misaligned due to translation, rotation, and scale [2]–[4]. The basic theory for translation estimation is the Fourier shift theorem [5]. Let I_1 and I_2 be the two images that differ only by a displacement (Δx, Δy)

$$I_1(x+\Delta x, y+\Delta y) = I_2(x,y). \tag{1}$$

The cross-power spectrum of two images I_1 and I_2 will be related by

$$\frac{\hat{I}_2(\omega_x,\omega_y)\hat{I}_1^*(\omega_x,\omega_y)}{\left|\hat{I}_2(\omega_x,\omega_y)\right|\left|\hat{I}_1^*(\omega_x,\omega_y)\right|} = e^{j(\omega_x\Delta x+\omega_y\Delta y)} \tag{2}$$

where $*$ denotes the complex conjugate. $\hat{I}_1$ and $\hat{I}_2$ are the Fourier transform of I_1 and I_2. The translation parameters (Δx, Δy) can be estimated by finding the maximum value position of the inverse FFT of (2).

When I_2 is a translated, rotated, and scaled replica of I_1

$$\begin{aligned} I_2(x,y) = I_1\,(s(x\cos\theta_0 + y\sin\theta_0) + \Delta x,\\ s(-x\sin\theta_0 + y\cos\theta_0) + \Delta y) \end{aligned} \tag{3}$$

where θ_0, s and (Δx, Δy) are the rotation angle, scale factor, and translation parameters, respectively.

The Fourier transform of (3) in polar coordinate systems is

$$\hat{I}_2(r,\theta) = e^{j(\omega_x\Delta x+\omega_y\Delta y)}s^{-2}\hat{I}_1(s^{-1}r, \theta+\theta_0) \tag{4}$$

where $\omega_x = r\cos\theta$, $\omega_y = r\sin\theta$. Let M_1 and M_2 be the magnitudes of $\hat{I}_1$ and $\hat{I}_2$; then, we have

$$M_2(r,\theta) = s^{-2}M_1(s^{-1}r, \theta+\theta_0) \tag{5}$$

$$M_2(\log r,\theta) = s^{-2}M_1(\log r - \log s, \theta+\theta_0). \tag{6}$$

Manuscript received June 22, 2005; revised July 26, 2005. This work was supported in part by the National Natural Science Foundation of China under Grant 60572152. The associate editor coordinating the review of this manuscript and approving it for publication was Prof. Lina J. Karam.

The authors are with the ICIE Institute, School of Electromechanical Engineering, Xidian University, Xi'an, China (e-mail: newopen1213@hotmail.com; blguo@xidian.edu.cn).

Digital Object Identifier 10.1109/LSP.2005.860549

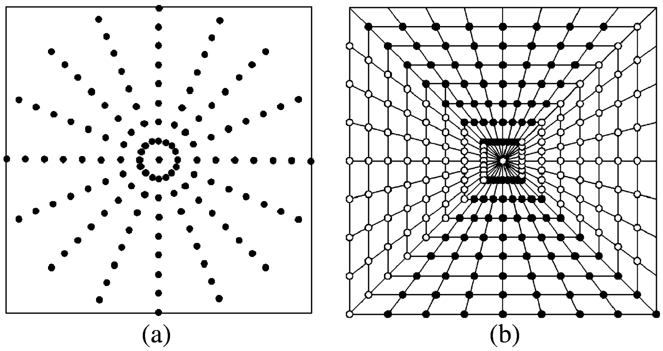

Fig. 1. Polar grid and pseudo-polar grid.

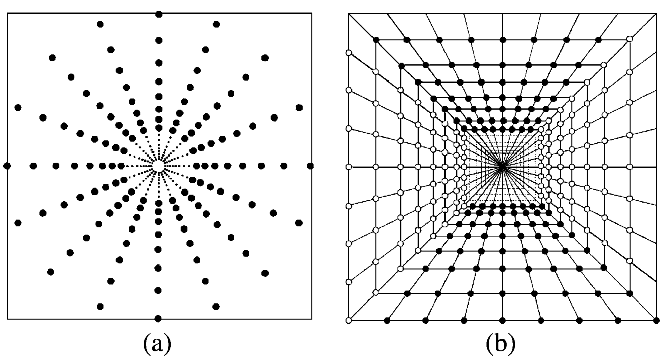

Fig. 2. Log-polar grid and pseudo-log-polar grid.

Letting $\xi = \log r$, $d = \log s$, (6) can be written as

$$M_2(\xi, \theta) = s^{-2} M_1(\xi - d, \theta + \theta_0). \tag{7}$$

Due to the fact that the Fourier spectrum is conjugate symmetric for real sequences, only two quadrants of the Fourier spectra of images are used to map them to log-polar plane for estimation parameters θ_0 and s. These parameters can be recovered by phase-correlation using (7). However, an ambiguity of π is in the estimation of the rotation angle [2]. This ambiguity is resolved by rotating I_2 according to both possibilities (θ_0 and $\theta_0 + \pi$) [4], scaling I_2 by the scale factor s, and finding the correlation peak of I_1 and I_2 for each possibility. The parameters corresponding to the highest correlation peak are chosen as the result.

Traditional algorithms are using 2-D FFT to approximate the log-polar Fourier representation of images. This will introduce large interpolation errors. Next, we will introduce the pseudo-polar and pseudo-log-polar coordinates to triumph over this disability.

III. Pseudo-Log-Polar Fourier Transform

The pseudo-polar Fourier transform proposed by Averbuch *et al.* [6] is based on a definition of a polar-like 2-D grid that enables fast Fourier computation. They used the concentric squares grid as an alternative to the polar grid shown in Fig. 1. The proposed PLPFFT algorithm approximates log-polar grid by pseudo-log-polar grid. These grids are shown in Fig. 2.

In general, for calculating the 2-D DFT on the integral Cartesian grid, Averbuch *et al.* define the horizontal and vertical frequencies

$$\left\{ \xi_x = \frac{2\pi k_1}{N}, \xi_y = \frac{2\pi k_2}{N} \right\}_{k_1,k_2=0}^{N-1}. \tag{8}$$

Then, we can get the familiar DFT in two dimensions by

$$\hat{f}(\xi_x, \xi_y) = \sum_{i_1=0}^{N-1} \sum_{i_2=0}^{N-1} f[i_1, i_2] \exp\left(-i(i_1\xi_x + i_2\xi_y)\right). \tag{9}$$

In a similar way, the pseudo-polar grid points can be defined in the frequency domain [6], which are separated into the basically vertical (BV) and the basically horizontal (BH) subsets. Fig. 1(b) depicts this grid, filled disks represent BV points, and circles denote BH ones. The BV group is defined by

$$\mathrm{BV} = \begin{cases} \xi_y = \frac{\pi l}{N}, & -N \le l < N \\ \xi_x = \xi_y \frac{2m}{N}, & -\frac{N}{2} \le m < \frac{N}{2} \end{cases} \tag{10}$$

and a similar definition describes the BH group.

Similar to pseudo-polar FT, we need to define pseudo-log-polar grid points in frequency domain. These points also separated as the BV and BH subsets. Fig. 2(b) shows these points. BV points are marked with the filled disks, and BH points are marked with circles. Next, a general representation is given by

$$\mathrm{BV} = \begin{cases} \xi_y = \pm \frac{\pi\rho}{N} \left(\frac{N}{\rho}\right)^{\frac{l}{(M-1)}}, & -\infty < l \le M-1 \\ \xi_x = \xi_y \frac{2m}{N}, & -\frac{N}{2} \le m < \frac{N}{2} \end{cases} \tag{11}$$

and

$$\mathrm{BH} = \begin{cases} \xi_x = \pm \frac{\pi\rho}{N} \left(\frac{N}{\rho}\right)^{\frac{l}{(M-1)}}, & -\infty < l \le M-1 \\ \xi_y = \xi_x \frac{2m}{N}, & -\frac{N}{2} \le m < \frac{N}{2} \end{cases} \tag{12}$$

where ρ is an important changeable parameter. For applications, $\rho \approx 1$ is a better option for stability. It determines the location of the log-polar coordinates origin in the Cartesian coordinates. If there is no special version, we let $M = 2N$ in (11) and (12) for the remainder of the letter. For calculating the value of $\hat{f}(\xi_x, \xi_y)$, a fast algorithm is needed. Since l is infinite, a limits $T \le l \le M-1$ should be added, where $T = \lfloor (1-M)(\log\sqrt{2}/\log(N/\rho)) \rfloor$. $\lfloor n \rfloor$ rounds the elements of n to the nearest integers toward minus infinity.

IV. Computation of Pseudo-Log-Polar FT and Log-Polar FT

Given the pseudo-log-polar grid points in the frequency domain, we are interested in computing the Fourier transform values. In what follows, we shall give a fast algorithm called the PLPFFT algorithm.

A. Computation of PLPFFT

Given the discrete signal X_k over the support $-N \le l < N$ and given an arbitrary scalar value α, the fractional FFT (FRFT) [8] is defined by

$$(F_\alpha X)_l = \sum_{k=-N}^{N-1} X_k \exp\left\{-i\alpha \frac{\pi}{N} lk\right\} \quad -N \le l < N. \tag{13}$$

Compared to the usual FFT, F_1 denotes the usual FFT, with F_{-1} denoting the usual inverse FFT (up to normalization). There is a highly efficient algorithm for FRFT by evaluating the Chirp-Z transform.

In our method, the processing of the BV and the BH data in the pseudo-log-polar grid are completely the same. The algorithm for BH points is easily obtained by switching the roles of the x and y axes. The following description will refer to the BV points only.

The computation of PLPFFT for BV points is based on the FRFT and the separability of 2-D DFT. The algorithm operates as follows.

1) Let I be the input image of size (n, m). $\tilde{I}$ is a zero-padded version of I such that $size(\tilde{I}) = (2N, 2N) = (2^k, 2^k)$, $k \in Z$, and $2N \geq s \cdot \max(n, m)$, $s \in Z$. Here, we let $s = 1$.
2) Apply the 1-D DFT in the y direction $\tilde{I}_{(\hat{x},i)} = DFT_X(\tilde{I})$. ξ_y the elevation direction frequencies are chosen by (11), where $T \leq l \leq M-1$. Because the Fourier spectrum is conjugate symmetric for real sequences, only the upper points are needed to compute.
3) Apply the FRFT operator to the rows of $\tilde{I}_{(\hat{x},l,i)}$ with a compression ratio of α_l

$$\mathrm{BV}_{l,i} = F_{\alpha_l}\left(\hat{I}_{(\hat{x},l,i)}\right), \quad i = 1, 2 \tag{14}$$

$$\alpha_l = \frac{\rho\left(\frac{N}{\rho}\right)^{\frac{l}{(M-1)}}}{N}, \quad T \leq l \leq M-1 \tag{15}$$

where $i = 1, 2$ denotes the upper points and lower points, respectively.

To evaluate DFT at BH points, we can reapply the above algorithm for the transposed version of image $\tilde{I}$.

B. Interpolation From Pseudo-Log-Polar DFT to Log-Polar DFT

Since the pseudo-log-polar grid is closer to the log-polar destination coordinates, there is a reason to believe that this approach will lead to better accuracy. The log-polar ones are obtained by two operations, similar to the polar ones in [6]. The interpolation from BV_1 points to log-polar grid is given as follows.

1) *Rotate the Rays:* In order to obtain an angularly uniform ray sampling as in the log-polar coordinate system, the term $2m/N$ in ξ_x is replaced by $\tan(\pi m/2N)$

$$\mathrm{BV}_1 = \begin{cases} \xi_y = -\frac{\pi\rho}{N}\left(\frac{N}{\rho}\right)^{\frac{l}{(M-1)}}, & -\infty < l \leq M-1 \\ \xi_x = \xi_y \tan\left(\frac{\pi m}{2N}\right), & -\frac{N}{2} \leq m < \frac{N}{2}. \end{cases} \tag{16}$$

This operation is equivalent to rotating rays $x = y \cdot 2m/N$ to rays $x = y \cdot \tan(\pi m/2N)$, which amounts to a 1-D linear interpolation operation along horizontal lines (for the BV_1 points). Similar to the polar ones, a set of N equispaced points along this line are also replaced by a new set of N unequispaced points along the same line in a different locations.

2) *Circle the Squares:* In order to obtain nonlinear increased concentric circles as required in the log-polar coordinate system, we need to "circle the squares." This is done by interpolating a set of $M-T$ points $(\xi_x, \xi_y)_{l,m}$ into a set of M points $(r_l,\, \theta_m)$ along each ray. Here, $(r_l,\, \theta_m)$ is represented by radial and angle. These points are

$$(\xi_x, \xi_y)_{l,m} = \left(-\frac{\pi\rho}{N}\left(\frac{N}{\rho}\right)^{\frac{l}{(M-1)}} \tan\left(\frac{\pi m}{2N}\right), -\frac{\pi\rho}{N}\left(\frac{N}{\rho}\right)^{\frac{l}{(M-1)}}\right) \tag{17}$$

where $T \leq l \leq M-1$, $T = \lfloor (1-M)\log\sqrt{2}/\log(N/\rho) \rfloor$. Also

$$(r_l, \theta_m) = \left(-\frac{\pi\rho}{N}\left(\frac{N}{\rho}\right)^{\frac{l}{(M-1)}}, \frac{\pi m}{2N}\right) \tag{18}$$

where $0 \leq l \leq M-1$. The destination points are located in concentric circles with a different spacing.

For BV_2 points and BH points, the same technique to approximate DFT at the log-polar grid is needed. By doing the up steps, we can obtain the DFT at log-polar points.

V. PLPFFT Registration Algorithm

In the log-polar Fourier domain, rotations and scalings are reduced to translations, which are estimated using phase correlation. Only the adjacent two quadrants of the PLPFFT of images are used to map them to the log-polar plane. This is because of the fact that the Fourier spectrum is conjugate symmetric for real sequences. The algorithm operates as follows.

1) The input images I_1 and I_2 are padded to $\tilde{I}_1$ and $\tilde{I}_2$ with sizes $(2^k,\, 2^k)$.
2) $I_1^{PLP}(\xi, \theta)$ and $I_2^{PLP}(\xi, \theta)$, the pseudo-log-polar DFT of $\tilde{I}_1$ and $\tilde{I}_2$, are calculated, respectively, where $\theta \in [-(\pi/4), (3\pi/4)]$.
3) The log-polar DFT $I_1^{LP}(\xi, \theta)$ and $I_2^{LP}(\xi, \theta)$ are approximated by $I_1^{PLP}(\xi, \theta)$ and $I_2^{PLP}(\xi, \theta)$, respectively. The polar axis and radial axis are approximated by linear interpolation.
4) The relative translation (s and θ_0) between $M_1^{LP}(\xi, \theta)$ and $M_2^{LP}(\xi, \theta)$ (the magnitude of $I_1^{LP}(\xi, \theta)$ and $I_2^{LP}(\xi, \theta)$) is recovered by a 2-D phase correlation on the polar and radial axes.
5) Let s and θ (θ_0 or $\theta_0 + \pi$) be the scaling value and the rotation angle estimated at 4), respectively. Then, the input image I_2 is scaled and rotated to be images I_{2,θ_0} and $I_{2,\theta_0+\pi}$.
6) Calculating the phase correlation peak for I_1 and I_2 (I_{2,θ_0} or $I_{2,\theta_0+\pi}$), respectively. Then, the parameters (θ, Δx, and Δy) corresponding to the higher correlation peak are chosen as the result.

Compared with PPFFT algorithm, PLPFFT has improved the accuracy of the log-polar DFT at low log coefficient points but reduced few at great ones. We can see that this technique has improved the detectability for estimating large translations, scalings, and rotations.

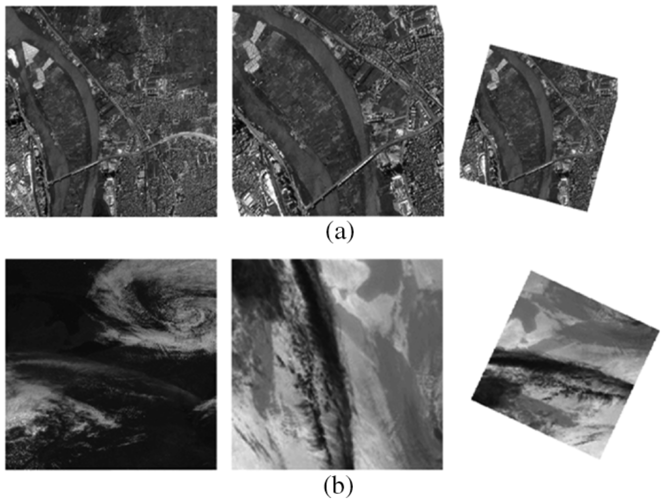

Fig. 3. Registration results of test images. (a) Single sensor images. (b) Multispectral images. Image enhancement and edge detection were preprocessed first.

TABLE I
REGISTRATION RESULTS OF IMAGE SETS IN FIG. 3

Images	Correct (Scale, θ)	Computed (Scale, θ)
a	(0.6536, 15°)	(0.6479, 14.9414°)
b	(0.6667, -65°)	(0.6711, -65.0391°)

VI. Experimental Results

This section presents the performance of the proposed registration algorithm for single sensor images, which were rotated, scaled, and translated to create the test pairs shown in Fig. 3(a). Registration of multispectral images was also examined in Fig. 3(b). This was done by a preprocessing step for images, such as image enhancement, edge detection, and target segmentation. In each row, the left and center images were registered. The results of transforming the center images by the transform parameters are shown in the right column. We present the numeric registration results for these images in Table I.

A comparing amount of FFT-, PPFFT-, and PLPFFT-based algorithms for registrations of images like Fig. 3 are given in Table II. Images of pairs 1 to 5 have a certain degree of overlap part. "$*$" represents the wrong testing result in Table II.

In Tables I and II, we can see that the proposed algorithm has certain robustness for images with partial alignment and can register multispectral images by some preprocessing. Compared to the conventional algorithms, our algorithm has a better ability for aligning images with large translations, rotations, and scalings. However, all the algorithms have boundary effects on images; sometimes we will get wrong results. This problem can be overcome in a certain extent by the method of windowing the images by some filtering windows.

TABLE II
REGISTRATION RESULTS BY PLPFFT AND CONVENTIONAL ALGORITHMS FOR IMAGES, SIMILAR TO THE ONES SHOWN IN FIG. 3

Images	Scale, θ	Peak value of Phase correlation for estimating scale and angle		
		PLPFFT	PPFFT	FFT
1	(1.5, 15°)	0.0548	*	*
2	(1.3, -21°)	0.0627	*	0.0871
3	(1, 15°)	0.2865	0.2652	0.1132
4	(1, 30°)	0.1581	0.1677	0.1150
5	(2, 75°)	0.1687	0.1694	0.0751

VII. Conclusion

This letter has presented a new image registration algorithm called PLPFFT for recovering large translations, rotations, and scaling factors between images. The proposed algorithm utilizes the pseudo-log-polar grid to approximate log-polar grid for improving the accuracy of the DFT at log-polar grid points. Compared to the conventional FFT-based registration algorithms, our algorithm shows a better performance for image registration.

References

[1] B. Zitová and J. Flusser, "Image registration methods: A survey," *Image Vision Comput.*, vol. 21, pp. 977–1000, Nov. 2003.
[2] B. S. Reddy and B. N. Chatterji, "An FFT-based technique for translation rotation, and scale-invariant image registration," *IEEE Trans. Image Process.*, vol. 5, no. 8, pp. 1266–1271, Aug. 1996.
[3] Q. S. Chen, M. Defrise, and F. Deconinck, "Symmetric phase-only matched filtering of Fourier–Mellin transform for image registration and recognition," *IEEE Trans. Pattern Anal. Mach. Intell.*, vol. 16, no. 12, pp. 1156–1168, Dec. 1994.
[4] Y. Keller, A. Averbuch, and M. Israeli, "Pseudopolar-based estimation of large translations, rotations, and scalings in images," *IEEE Trans. Image Process.*, vol. 14, no. 1, pp. 12–22, Jan. 2005.
[5] C. D. Kuglin and D. C. Hines, "The phase correlation image alignment method," in *Proc. IEEE Conf. Cybernetics Society*, Sep. 1975, pp. 163–165.
[6] A. Averbuch, R. R. Coifman, D. L. Donoho, M. Elad, and M. Israeli, "Fast and accurate polar Fourier transform," *SIAM J. Sci. Comput.*, submitted for publication.
[7] ——, "Accurate and fast discrete polar Fourier transform," in *Proc. 37th Asilomar Conf. Signals, Systems, Computers*, Pacific Grove, CA, 2003, pp. 1933–1937.
[8] ——, "Fast Slant Stack: A notion of Randon transform for data in a Cartesian grid which is rapidly computible, algebraically exact, geometrically faithful and invertible," *SIAM J. Sci. Comput.*, to be published.